Biological Cybernetics (2019) 113:61–70
https://doi.org/10.1007/s00422-018-0771-0

Biological Cybernetics

REVIEW

Controlling excitable wave behaviors through the tuning of three parameters

Sayak Bhattacharya[1] · Pablo A. Iglesias[1]

Received: 26 January 2018 / Accepted: 12 July 2018 / Published online: 28 July 2018

Abstract
Excitable systems are a class of dynamical systems that can generate self-sustaining waves of activity. These waves are known to manifest differently under diverse conditions, whereas some travel as planar or radial waves, and others evolve into rotating spirals. Excitable systems can also form stationary stable patterns through standing waves. Under certain conditions, these waves are also known to be reflected at no-flux boundaries. Here, we review the basic characteristics of these four entities: traveling, rotating, standing and reflected waves. By studying their mechanisms of formation, we show how through manipulation of three critical parameters: time-scale separation, space-scale separation and threshold, we can interchangeably control the formation of all the aforementioned wave types.

Keywords Excitable systems · Wave propagation · Spiral waves · Standing waves · Wave reflection

1 Introduction

Traveling excitable waves were first observed on the giant squid axon by Hodgkin and Huxley [20] in their groundbreaking study of the neural action potential. Their Nobel prize-winning work gave birth to the idea of excitability, a form of ultrasensitivity born through the coupling of activators and inhibitors. As the name suggests, an excitable system can be triggered when an input crosses a threshold for activation resulting in a sharp rise and fall in activity. Because subthreshold inputs do not elicit any response, this behavior is characterized as an all-or-nothing type response. This excitatory jump is followed by a refractory period, together creating an isolated peak of activity. If this peak is able to trigger adjacent regions in a medium, it forms a propagating wave front. Excitable wave propagation has been shown to be prevalent in many biological systems including neural synapses in the motor cortex [55], cortical waves during cytokinesis of *Xenopus* oocytes [1], calcium waves in the cardiac myocyte [6,63] and actin polymerization waves in migratory cells [10,60]. For more examples of wave propagation in biological systems, see the recent review by [9].

It is intuitive to think about waves as traveling entities. However, both theoretical and experimental studies have shown the existence of standing waves in which the peak of activity does not spread in space but remains localized at a persistent high, creating spatial patterns [44]. That activator–inhibitor systems can generate stable patterns has been known for a long time, most notably through the work of [56] and Gierer–Meinhardt [19]. In recent years, the idea that traveling waves may transform into standing waves to create sustained patterns has also been suggested [41,59]. Although the above systems are not by-definition excitable, they are all activator–inhibitor systems that display ultrasensitivity or a diffusion-driven instability. Typical excitable systems have also been shown to sustain stable standing wave solutions [13], most famously through manipulations of the Belousov–Zhabotinsky reaction [58].

Besides traveling and standing waves, rotating spiral waves are a subject of significant research interest, owing to their relevance in cardiac arrest [8,24,28]. Excitable media

Communicated by Peter J. Thomas.

This work was supported by DARPA under contract number: HR0011-16-C-0139.

This article belongs to the Special Issue on *Control Theory in Biology and Medicine*. It derived from a workshop at the Mathematical Biosciences Institute, Ohio State University, Columbus, OH, USA.

✉ Pablo A. Iglesias
pi@jhu.edu

Sayak Bhattacharya
sbhatt11@jhu.edu

[1] Department of Electrical and Computer Engineering, The Johns Hopkins University, Baltimore, USA

have been shown to sustain spiral waves when a wave break occurs and multiple mechanisms, both theoretically and experimentally, have been proposed to account for their generation [48,51,67]. These mechanisms have led to better clinical procedures such as localized tissue ablation and numerous other control strategies to be able to eliminate spirals and restore normal rhythm during atrial fibrillation [34,35,47,62]. Spiral waves have also been implicated in a variety of other processes such as memory consolidation [43] and spreading depression in the chicken retina [7].

The reflection of excitable waves has also received some attention through numerical simulations and chemical systems. It has been suggested that waves being transmitted in excitable cables may undergo reflection through the variations of cable diameters or excitability levels [14]. Chemical wave reflection has been observed in the Zhabotinsky reaction with wave speed heterogeneity in different media [65].

The wide spectrum of wave behavior consisting of traveling waves, standing waves, spiral waves and reflected waves can all be placed on a bifurcation diagram using certain critical parameters of the excitable system, namely the time-scale separation, the space-scale separation and the threshold for activation. Here, we use a simple two-dimensional model to show the relevance of these parameters and illustrate how all these behaviors can be generated through manipulation of the aforementioned critical parameters of the system.

2 The model and the traveling wave

One of the earliest models of excitable systems is Lapicque's integrate-and-fire model [31]. The Lapicque model proposes that the membrane voltage integrates inputs for infinite time until a threshold is crossed. Over the years, the basic idea of supra-threshold firing has remained the same, but the mechanism of threshold crossing has changed. Though the concept of time-dependent memory was added later to create the "leaky" integrate-and-fire model, the Hodgkin–Huxley model garnered more popularity owing to accuracy from experimental validations. Since then excitable models have been simplified from the four-dimensional Hodgkin–Huxley to the widely used two-dimensional FitzHugh–Nagumo (FHN) model [17,46] or, later, the Morris–Lecar model [42].

Throughout this review, we illustrate our concepts using a model used to describe the excitable behavior observed during cell migration [2]. Inspired by the FHN model, it is two dimensional, consisting of an autocatalytic activator and a delayed inhibitor (Fig. 1a). Describing their levels of activity by u and v, respectively, the system obeys the following two partial differential equations:

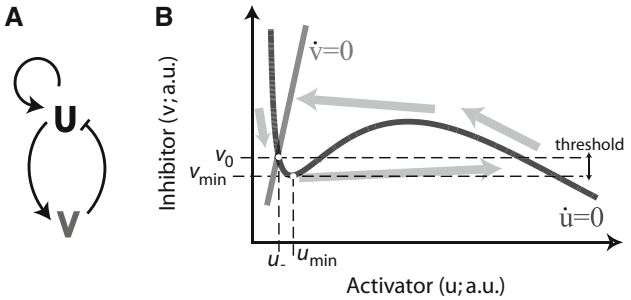

Fig. 1 Activator–inhibitor model used to illustrate excitability. **a** The two-species activator(u)–inhibitor(v) model showing positive and negative feedback loops. **b** Phase-space representation showing the critical points and threshold. The activator ($\dot{u} = 0$) and inhibitor ($\dot{v} = 0$) nullclines are drawn with the gray arrows showing the phase excursion corresponding to an excitation spike response

$$\frac{\partial u}{\partial t} = D_u \nabla^2 u - a_1 u - a_2 u(v - r) + \frac{a_3 u^2}{a_4^2 + u^2} + B \tag{1a}$$

$$\frac{\partial v}{\partial t} = D_v \nabla^2 v + \varepsilon(-v + c_{th} u) \tag{1b}$$

The incorporation of the diffusion terms moves us away from the ordinary differential equations of Hodgkin–Huxley, where interaction between adjacent neurons was achieved through synaptic connections that served as input terms in the activator equation [5]. Instead, spatial connections are formed by adding diffusion terms using uniform coefficients in a discretized system.

A classic characteristic of the excitable system is an all-or-nothing response where subthreshold values of the activator are quickly subdued by the degradation terms of (1a). However, once the activator concentration becomes large enough for the nonlinearity to take effect, a significant rise in the activator is obtained. The slow response of the inhibitor is incorporated through the variable $\varepsilon \ll 1$ which describes the time-scale separation between the two components. This causes the inhibitor levels to increase with a delay when compared to the activator, allowing the activator to rise sharply through positive feedback, described by the Hill function with exponent two, creating the wave "front." This time-scale separation is also responsible for the refractory period of the system. After the inhibitor has subdued the activator, there is a window of time where the inhibitor slowly degrades, creating a zone of high inhibition during which no further activity can take place. This period of inhibitor decay is determined by ε and defines the wave "back."

The dynamics of the excitable system are better visualized in phase plane where the threshold of the system can be approximated by the vertical distance between the equilibrium set point (u_-, v_0) and the minimum of the activator nullcline $(u_{\min}, v_{\min})$ [2] (Fig. 1b). An external input to the excitable element is modeled through the input variable r and through the diffusion term, both serving to raise the

activator nullcline and lowering the threshold of the system. Lowering the slope c_{th} of the inhibitor nullcline is another way to decrease this threshold. A displacement of the initial state, sufficient to clear this threshold, results in an excursion around the phase space (Fig. 1b) generating a spike in activity in one excitable element. This spike leads to a wave front in the spatial dimension, triggering the neighboring excitable elements to propagate in space, creating a traveling wave.

It is important to note that in this context, the traveling wave refers to an up- and down-change in an activity that propagates in space. Technically, the down-jump is not necessary for a wave to spread and this would correspond to a bistable wave, more along the lines of what [41] proposed. For the purposes of this paper, the traveling wave we refer to is in fact a "pulse" that travels in space, made possible by the inhibitor/refractory variable [21].

Excitable waves propagate radially outward from a single point. Once the propagation begins, the wave cannot spread inward owing to the presence of the inhibitor (refractory period) just behind it. One can think of a traveling wave as the activator (wave front) spreading with the inhibitor (wave back) chasing it [23]. A well-known and interesting characteristic of traveling waves is their annihilation on collision. This is the result of the inhibitor "catching up" to the activator as the wave front runs out of room to spread on encountering another wave front.

Figure 2a illustrates the basics of wave propagation. Each white square is an excitable element that, when triggered, has high activator (u; dark gray). This is followed by a refractory period where the concentration of the inhibitor is high (v; light gray), after which the element goes back to the resting state (white). Together, unidirectional wave propagation can be ensured, as shown in Fig. 2b, as the activator cannot spread toward the left as the elements behind it are in the refractory state. Similarly, annihilation on collision represents a situation in which the activator cannot spread in either direction owing to the refractory regions of the original wave on one side and of the colliding wave on the other (Fig. 2c).

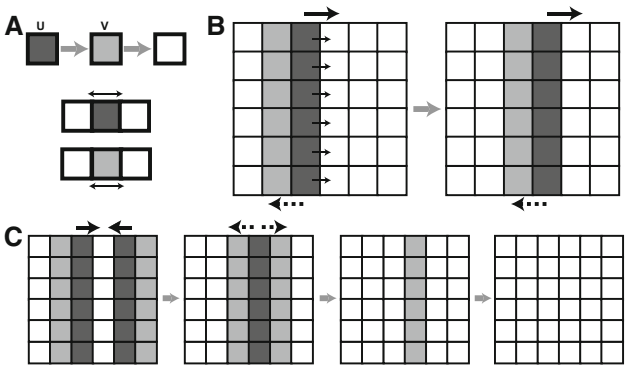

Fig. 2 Wave propagation and annihilation. **a** The possibilities during wave propagation. (top) An element with high u (dark gray) will change to high v (light gray) and then return to steady state (white). (bottom) Both u and v can diffuse to adjacent elements. **b** Unidirectional wave propagation (solid arrow) occurs as the activator cannot diffuse to the left (dashed arrow) because of the presence of the inhibitor. Here, it is assumed that the inhibitor cannot diffuse. **c** Wave annihilation owing to the surrounding of the activator by the inhibitor upon collision (second panel)

So far we have talked about the time-scale separation (ε) and the threshold ($v_0 - v_{\min}$). The third critical parameter is the space-scale separation, i.e., the ratio D_v/D_u. Traveling waves are most commonly observed when the space-scale separation is such that $D_v/D_u \approx 0$ for reasons that we explain later in the paper. This signifies that the level of the inhibitor is constant (v_0) across the wave front as the wave propagates and is only high at the wave back. Ideally, both the activator and inhibitor should diffuse across excitable elements (Fig. 2a). For the $D_v/D_u \approx 0$ assumption, we assume that the inhibitor cannot diffuse. If this assumption does not hold, it is obvious that whether the wave will propagate will depend on the relative rates of propagation of u and v.

3 Wave velocity and threshold

The velocity of this wave front has been the subject of extensive research, typically using singular perturbation approaches [26,52,57]. In one-dimensional space, it can be proved that the wave velocity (w_{1D}) is completely determined by the initial level of the inhibitor, also called the controller species [15]. The velocity is given by Luther's equation [45,53]:

$$w_{1D} = m(v_0)\sqrt{kD_u}$$

where $m(v_0)$ is the wave velocity determining function, dependent on the initial set point v_0, D_u is the diffusion coefficient of the activator and k is a first-order rate constant for the autocatalytic production of the activator in response to suprathreshold perturbations. The function $m(v_0)$ is inversely proportional to v_0, i.e., a higher threshold leads to a slower wave velocity and vice versa. For a constant set of parameters for the activator nullcline, the excitability threshold ($v_0 - v_{\min}$) is controlled by the initial inhibitor level. For this reason, we use the terms v_0 and threshold interchangeably throughout this paper. More particularly, to control the threshold we modulate the slope of the inhibitor nullcline through the parameter (c_{th}).

While the theory of wave velocity in one dimension is controlled by the threshold, in two spatial dimensions both the initial threshold (v_0) and the local wave curvature (κ) are critical for the wave speed (w_{2D}) determination [16,27,

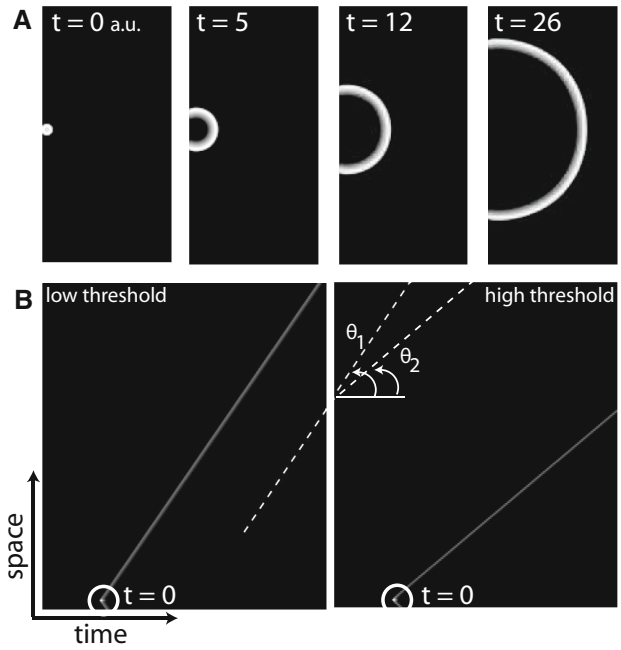

Fig. 3 The traveling wave. **a** Evolution of a wave front after a point trigger at $t = 0$. Time units are arbitrary. **b** Kymographs (plotting activity over 1D space and time) showing the traveling wave (gray solid line) at a low threshold (left) and a high threshold (right). The trigger element at $t = 0$ is marked. The dashed lines are lines parallel to the wave front. These are used to compare the slopes of the waves, i.e., the wave velocity. $\theta_1 > \theta_2$ indicates that the low threshold wave travels faster

66]. In this case, the wave velocity is given by the eikonal equation:

$$w_{2D} = m(v_0) + \varepsilon\kappa \tag{2}$$

For a constant time-scale separation ε, the wave velocity is given by the threshold of the system adjusted for curvature. That is, a wave that curves away from the direction of propagation ($\kappa < 0$) is slower than a plane wave ($\kappa = 0$) at the same initial threshold level.

3.1 A slower wave in a high threshold domain

In Fig. 2, we illustrated the wave dynamics using a simple cartoon depicting a planar wave. Stimulation of a point in space actually results in a radial wave, as shown through simulations in Fig. 3a. These simulations were done in MATLAB, using a discretized domain where a wave was initiated by stimulating one point in space (transiently increasing r in (1a) at a point). Diffusion is simulated through the central difference approximation. The parameters for simulation are given in Tables 1 and 2 . Simulation codes will be provided upon request.

One-dimensional simulations at two different thresholds provide a clear idea as to the different wave velocities. These

Table 1 Nominal simulation parameters

Parameter	Value
a_1	0.167
a_2	16.67
a_3	167
a_4	1.2
B	1.47
Δx	0.1
Grid size (1D)	400
Grid size (2D)	200 × 200

Table 2 Critical parameters for various wave patterns

Wave type	c_{th}	D_s (D_v/D_u)	ε
Traveling	30 (fast) 60 (slow)	$10^{-2}(10^{-3}/10^{-1})$	0.15
Spiral	30	10^{-2} ($10^{-3}/10^{-1}$)	0.15 (low curl) 0.20 (high curl)
Stop	30	3.2 (0.32/0.1)	0.03
Standing	30	20 (2.0/0.1)	0.03
Reflecting	10	1 (1.0/1.0)	0.03

are shown through kymographs where the activator levels are plotted across space (y-axis) and time (x-axis). In this case, the propagation speed is determined by the slope of the wave front as shown in the kymographs. Two-dimensional simulations are harder to judge for velocity owing to the time-lapse videos. However, simulating two waves at two thresholds and comparing the slopes of the resulting wave front shows clearly how the low threshold wave travels faster (Fig. 3b).

3.2 Wave stopping at inexcitable thresholds

So far we have been concerned about wave velocities in high threshold regions where the excitation threshold is sufficiently low for the activity of one element to trigger its neighbor. The presence of inexcitable regions where v_0 is high causes the wave to stop at the boundary and not propagate inside the region. This is because the activity from one element is not sufficient to clear the threshold ($v_0 - v_{\min}$) of the neighboring element—creating a wave break.

Noteworthy at this point is that with our chosen parameters, wave stopping can only occur when an inexcitable element is reached. In cases where $D_v/D_u \gg 1$, wave stopping may naturally occur owing to a rise in the inhibitor level in the surrounding as the wave propagates [41]. Because of this long-ranging inhibitor, an inexcitable region may naturally get created in space causing the wave to stop. However, whenever $D_v/D_u \approx 0$, natural wave stopping is not pertinent.

4 Traveling wave to a rotating wave

When the traveling wave encounters an inexcitable obstacle, the end of the wave gets anchored and the wave keeps rotating around the obstacle [61]. This mechanism of rotating wave generation is perhaps the most common in experimental literature where people have introduced blockages alongside a wave pacemaker to create rotating waves [48,51]. Varying the degrees of anisotropy (such as introducing different sized obstacles) in the medium can generate different spiral waves [49]. Recently, an anchoring mechanism has been proposed without the use of an obstacle but instead through a fast propagation region (FPR), where the diffusion rate of the activator is altered to create a heterogeneous velocity zone [67]. In this case, the wave spirals using the FPR as a core.

A spiral wave is essentially a broken traveling wave that has increased curvature at the central core. Any sort of anisotropy in the medium can be thought of as a tool to alter the curvature of the wave tip. If the tip of the wave is curled, then the rest of the wave tries to normalize the high curvature of the core, resulting in gradually increasing curvature as one moves toward the central tip. This results in each subsequent point on the spiral rotating in concentric circles around the central core—which itself is rotating in the smallest circle. This is the definition of a standard one-armed Archimedean spiral with a rotating center [44,63,64].

Thus, even without a visible anchor, a spiral wave can arise if a broken plane wave curls at its tip. It has been shown that in homogenous excitable media, if the system is "strongly excitable" [40]—which in this context can be thought of as $D_v/D_u \approx 0$, then a broken wave will automatically start to curl. This can be tested using a transient threshold heterogeneity that arrives suddenly in the path of a traveling wave. Owing to this inexcitable heterogeneity, the wave breaks. After the wave break, if the media is homogenized, we are left with a broken traveling wave.

Owing to the abrupt ending of the wave back, the broken end of the wave front expands outward "curling" around the back. Figure 4a shows how a broken wave develops a curl owing to the additional diffusion direction made available owing to the wave break. This creates a "kink" at the tip of the wave where the tip has a higher curvature than the rest of the wave. This kink at the end of the wave causes the tip of the wave to evolve differently than the rest of the wave (Fig. 5). The velocity of the wave in region z_α (Fig. 5) is given by:

$$w_\alpha = m(v_\alpha) + \varepsilon\kappa_\alpha$$

In the region z_δ, the presence of the kink changes both the threshold and curvature terms in the velocity equation. In particular, the kink adds a large negative curvature (κ_δ, where

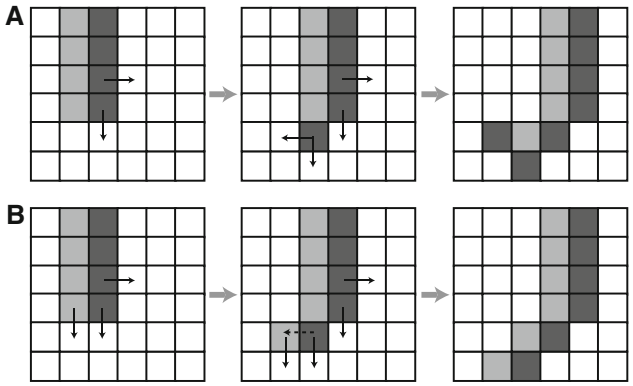

Fig. 4 Cartoon depicting the formation of spiral waves. **a** Assuming that the inhibitor (light gray) cannot diffuse, the relevant diffusion directions are shown through solid arrows. **b** Inhibitor diffuses along with activator (dark gray). The dashed arrow indicates where diffusion is not possible

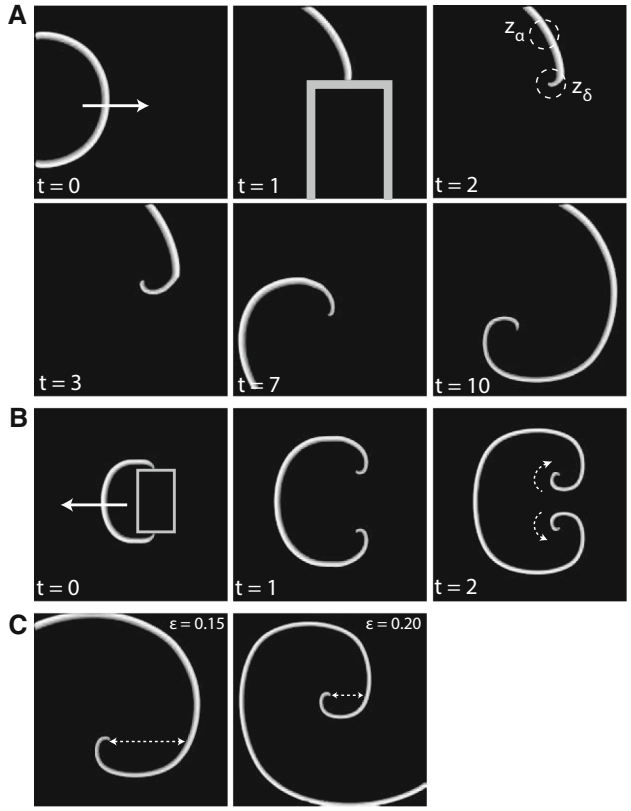

Fig. 5 Formation of spiral waves. **a** The $t = 0$ panel shows a traveling wave that is not broken. At $t = 1$, an inexcitable obstacle (gray box) that the wave cannot penetrate is introduced, resulting in a wave break. The block is removed at $t = 2$ and the regions z_α and z_δ have different curvature. This difference in curvature evolves to create the spiral. **b** Introduction of a threshold block (gray box) in the middle of the wave ($t = 0$) generates two spiral tips of opposite chirality (dashed arrows, $t = 2$). **c** Comparing two spirals of different time-scale separation. The dashed arrow is used to demarcate the distance between the tip and the nearest rotating arm. The line is drawn at an instant when both spiral tips are at the same phase. The line is extended until a rotating arm is encountered. For a higher time-scale separation (right panel), this distance is smaller indicating a spiral with a higher curl

$\kappa_\delta < \kappa_\alpha$) to the wave velocity equation. Moreover, because of the kink, the tip of the wave is now closer to the refractory zone of the wave back where the threshold is significantly higher (v_δ, where $v_\delta > v_\alpha$).

Thus, the wave velocity in region z_δ can be written as:

$$w_\delta = (m(v_\delta) + \varepsilon\kappa_\delta) < w_\alpha$$

This causes the tip of the wave to move more slowly than the rest of the wave after the threshold block is removed. As a result, this creates an even higher curvature wave tip that is slower. Ultimately, this causes the wave tip to merge with the wave back that is immediately adjacent to it creating a phase singularity. Together, the slower velocity of the tip and the increasing velocity as one moves away from the tip initiates a spiral wave.

It is interesting to note here that if the high threshold block is placed in the middle of the traveling wave, two wave tips are exposed once the block is removed. Both these wave tips curl to form a spiral wave—each rotating in opposite directions, i.e., spirals of *opposite chirality* (Fig. 5b). The height of the block must be sufficient such that the two tips do not annihilate each other before the spirals can evolve.

4.1 Controling spiral radius through the modulation of the time-scale separation

The wave velocity equation (2) is dependent on ε. Increasing ε has two main effects. First, it increases the contribution from curvature, resulting in a sharper kink at the edge of the wave. This causes the wave to turn more sharply as compared to a lower ε—effectively shrinking the spiral radius. Second, the refractory period of the wave back decreases with increasing ε. This also brings the spiral arms closer together as the wave back is reduced. Figure 5c compares two simulated spirals with different values of ε, thus showing how the time-scale separation can be used to control the resulting spiral radius.

The refractory period—controlled by the time-scale separation ε has an important influence on the motion of the tip of the spiral. In the event that the rotation period of the spiral arms is large, the recovery time of the medium does not influence the incoming arm of the spiral [39]. However, if the period of rotation becomes comparable with the recovery time, the spiral tip meanders in excitable space. There are different modes of meandering spiral tips such as epicycloid-like and hypocycloid-like [54], with the extent of meandering depending upon the excitability of the medium. The transition between meandering behaviors has also been chemically explored through light-sensitive modulation of excitability in the Belousov–Zhabotinsky reaction [3,33].

A traveling wave thus can turn into a spiral wave if it is broken, as a broken wave has a tendency to curl in strongly excitable media. The extent and speed of the curl can be controlled using the time-scale separation as ε controls the length of the wave back, around which the front curls. Coming back to the space-scale separation, as $D_v/D_u \approx 0$ was assumed, the curling of the wave was easy. One can imagine for higher ratios of the space-scale separation the inhibitor will diffuse into the empty region beside the broken wave tip making it difficult for the wave to curl (Fig. 4b). Hence, for higher values of D_v/D_u, the system becomes weakly excitable resulting in a low-curl spiral or no spiral evolution [40] owing to wave stopping, which we discuss next.

5 A large space-scale separation: wave stopping, standing and reflected waves

As we move away from the approximation of a low D_v/D_u and increase the space-scale separation, a number of interesting behaviors are obtained. A large value of D_v/D_u implies that as the wave propagates, the level of inhibition in the surrounding region will not remain constant at v_0, but will rather increase, thus competing with the activator propagation. A natural corollary of this is that the subsequent triggers of the wave front occur at increased threshold levels as the wave spreads. A higher threshold corresponds to a lower wave velocity, and thus the wave slows down as it propagates. As more and more inhibitor accumulates in the medium, the inhibition level reaches a critical threshold $v^\star$ where:

$$m(v^\star) = 0,$$

i.e., recalling Luther's equation for wave velocity (w):

$$w = m(v^\star)\sqrt{kD_u} = 0$$

Thus, the wave slows down, which is reflected as a curved wave on the kymograph (Fig. 6a), and ultimately stops when the critical threshold is reached. This phenomenon is similar to the wave-pinning mechanism proposed for bistable reaction-diffusion systems [41], with the only difference being that no actual "pinning" occurs owing to the excitable response.

It is worthwhile to note at this juncture that owing to the inherent slowness of the inhibitor decay, the resting time of the inhibitor in space is higher than that of the activator. This allows greater dispersion of the inhibitor in space, even for the same diffusion coefficient. Hence, the notion that $D_v/D_u \gg 1$ is not a necessary condition for wave stopping in systems where the lifetime of the inhibitor is significantly

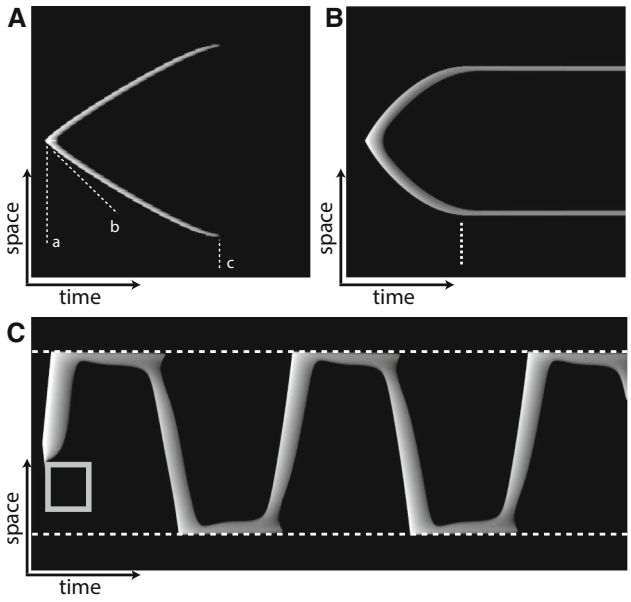

Fig. 6 Stopped wave, standing wave and the reflected wave. **a** A stopped wave kymograph where the wave triggers at "a," curves as it slows down (the dashed line "b" acts as a spatial fiduciary to illustrate the curving) and finally stops as "c." **b** The standing wave kymograph with the dashed line showing where the traveling wave transforms into a stable standing wave. **c** The reflected wave kymograph with the dashed lines demarcating the no-flux boundary. The initial threshold block is shown through the gray box

greater than that of the activator. For small time-scale separation values (approaching the singular limit), $D_v/D_u \gg 1$ becomes relevant to compensate for the delay in the inhibitor build-up.

5.1 Standing waves

For a sufficiently high space-scale separation, excitable systems can produce stable standing pulses [12,18,25]. Theories of pattern formation, laid down by [56] and Meinhardt [19] suggest that a long-ranging inhibitor, coupled with a local autocatalytic activator can result in a system with a low homogenous equilibrium state to spontaneously change into a higher stable state to form a stable pattern. While Turing's theory is diffusion driven, Meinhardt's is reliant on lateral inhibition. However, both require high space-scale separation between the activator and inhibitor components.

Fast diffusion of the inhibitor in the surrounding space can limit the propagation of the activator. While in moderate D_v/D_u cases, this results in wave stopping, and for sufficiently high space-scale separation, this creates a stable peak in space—called a standing or stationary wave. Ermentrout et al. [13] show how this occurs through lateral inhibition when the ratio of the time- and space-scale separation is small. In fact, traveling and standing waves can coexist near a bifurcation zone and changing the space-scale separation can cause the system to switch between the two states [11]. Some researchers also suggest that this occurs through a subcritical Turing-type bifurcation [4]. Common to both mechanisms is a change from a homoclinic orbit to a heteroclinic orbit between low and high equilibrium states that creates a stable standing wave.

For the model parameters that we have chosen, the Turing instability is not pertinent as the conditions for diffusion-driven instability [32] are not satisfied. Instead, we show an example of a standing wave where the heteroclinic orbit develops owing to lateral inhibition causing a stable standing wave to develop when the wave stops, more along the lines of what Ermentrout and colleagues proposed. By simulating the system with a low value of ε/D_s, where ε is the time-scale separation and $D_s = D_v/D_u$ is the space-scale separation, we achieve a stable standing wave when the wave stops (Fig. 6b).

5.2 Reflected waves

Before we consider reflected waves, it is useful to recall the possible bifurcations in the model under consideration [2,22]. The equilibrium that was chosen (u_-, v_0) is asymptotically stable, i.e., small perturbations cause an immediate return back to steady-state without any appreciable response. However, as the definition of excitable systems dictates, a large amplitude response exists when the input crosses a certain threshold. This occurs because the equilibrium is close to a Hopf bifurcation point $(u_{\min}, v_{\min})$ (Fig. 7a). If the state were to cross this minimum, a response would be obtained. Extending this idea further, if the threshold of the system (slope of inhibitor nullcline, c_{th}) were to be lowered beyond the bifurcation point, the steady-state would be rendered unstable and a large amplitude limit cycle would arise. At this situation, any and every perturbation (positive or negative) is sufficient to trigger a response (Fig. 7b).

As mentioned earlier, reflection of waves can be brought about through inhomogeneities in the medium. Even without inhomogeneities, if a no-flux boundary exists, waves can be reflected at a high space-scale separation if the threshold is lowered beyond the critical Hopf bifurcation point [30]. More particularly, in such a situation, a traveling wave will stop at the no-flux boundary—create a standing wave—and then get reflected back. Because of the instability around the Hopf equilibrium, any transient activity near the boundary will re-initiate the traveling wave—this time in the opposite direction. Once the standing wave is formed, transients are generated through the dissipation of the inhibitor that can trigger adjacent activator elements provided the refractory period is over. Note that inhibition triggering a response from the excitable system can only occur in the Hopf bifurcation situation.

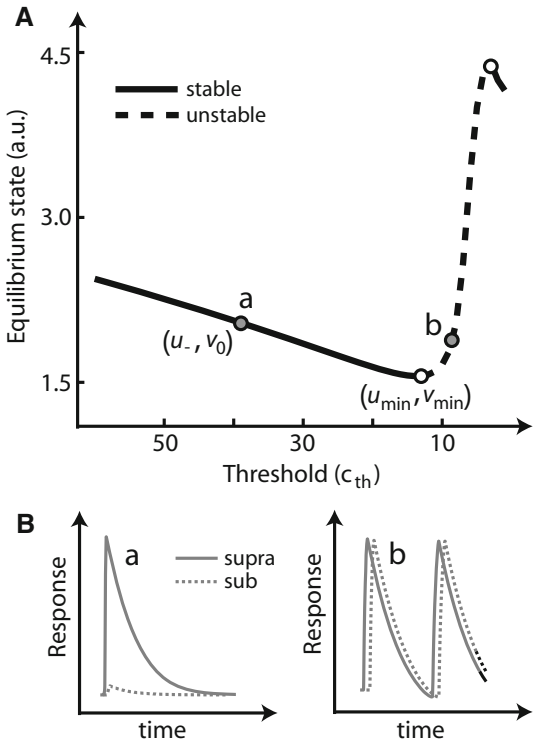

Fig. 7 Biifurcation diagram for the excitable system as a function of the slope, c_{th}, of the inhibitor species. **a** Bifurcation diagram indicating the stability of the equilibrium state as the threshold parameter is varied. The Hopf bifurcation point, where the stability changes, is demarcated by the white circle. **b** Responses to sub- and supra-threshold stimuli at the equilibria a and b (gray circles) from panel A. The response to a stable equilibrium (a, left) differs depending on the input stimulus, while the response at an equilibrium past the bifurcation point (b, right) is oscillatory irrespective of the input. A phase shift has been added for illustration purposes only

We simulated the no-flux boundary by limiting the diffusion of the activator beyond a boundary. We used a threshold block on one side of the trigger to ensure that the wave travels toward one boundary at a time (otherwise, they would annihilate upon collision after reflection) (Fig. 6c). With the whole system being inside the Hopf bifurcation zone, the wave traveled to one boundary and formed a standing wave owing to the high space-scale separation. Because of the transients, however, a reflected wave is generated once the refractory period subsides—breaking the standing wave with it. Whether the standing wave will break or not depends on the stability of the standing pattern, which can be modulated through the ratio of the time- and space-scale separation [13].

It is interesting to note that excitable wave reflection is counter-intuitive as the inhibitor is constantly behind the activator wave front. Hence, it is necessary for the zero flux boundary to cause the wave to stop, allowing sufficient time for the inhibitory refractory period to dissipate. There are other methods to generate reflected waves such as through reactant depletion at the wave front [50] but, even in that case, the wave has to stand at the boundary long enough for the medium to recover. Moreover, though in the simulations, the whole system was assumed in the Hopf bifurcation zone, in reality only the boundary regions need to be at such a low threshold. Within the interior, wave speed may be modulated through threshold manipulation as illustrated in earlier sections.

6 Discussion

Wave propagation is a characteristic hallmark of excitability. The fact that excitable waves can change their behavior depending on initial conditions is of utmost importance to studying various physiological phenomena. Here, we illustrated that through the manipulation of the time-scale separation, space-scale separation and threshold one can control the observed wave pattern. Note that we talked only about mechanisms that require either none or minimal parameter changes other than those to the critical parameters described above.

All the results are summarized in the flowchart shown in Fig. 8. The terms "low," "high," etc., are used in a qualitative sense with the understanding that for a system to be excitable, the time-scale separation and threshold should be low to begin with. The reader should reference the table of simulation parameters for a reasonable estimate (Tables 1, 2). The flowchart emphasizes how manipulating three parame-

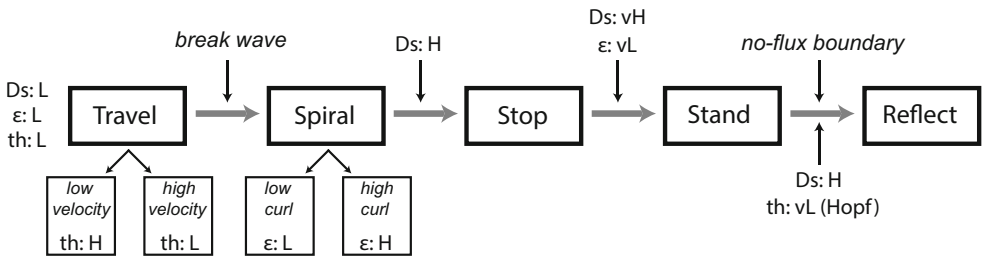

Fig. 8 Scheme to control wave behaviors. L, vL, H and vH denote low, very low, high and very high, respectively. $D_s = D_v/D_u$ denotes the space-scale separation, ε is the time-scale separation and th is the threshold parameter c_{th} from the inhibitor equation

ters (with added conditions in some cases), allows one to switch between wave behaviors.

Low space-scale separations lead to traveling waves. The velocity of these waves can be altered by modulating the threshold or the time-scale separation, again with the understanding that too high a threshold or ε would result in inexcitability. Breaking a traveling wave through a high threshold obstacle can create a rotating spiral wave. Again, the radius or velocity of the spiral wave can be altered by altering the time-scale separation parameter. For high space-scale separations, the traveling waves and spirals are lost as wave stopping occurs. These stopped waves may form standing waves or stable patterns if the ratio between the time and space-scale separation is sufficiently small. Lowering of the threshold beyond the Hopf bifurcation point, with a no-flux boundary condition can create reflected waves as well.

While we split these wave behaviors into zones of high or low parameters, there are parameter zones in which these wave types coexist. Many studies have gone into deconstructing the effects of time- and space-scale separations as driving parameters are slowly varied [11,59]. Though there are other combinations of these parameters that cause the same transitions, we have reviewed only those combinations that best illustrated the wave dynamics.

The usefulness of studying such wave types are diverse as these are predictions into how modulating some parameters can drastically change wave properties and the resultant species function. Recently, we showed theoretically and experimentally that by altering the threshold of the excitable cell migration network, wave propagation characteristics could be changed and that these translated to significantly different migratory modes [38]. Specifically, lowering the threshold significantly increased wave velocity and range and these changes transformed amoeboid cells into fan-shaped or oscillatory cells. These insights may lead to therapeutic applications for cancer cells as the migration characteristics of tumor cells is critical during metastasis. Standing waves have been extensively probed in chemical setups such as the Belousov–Zhabotinsky reaction. Turing patterns have been hypothesized on the angelfish [29], while Turing's main prediction [56] for pattern formation through morphogen gradients in the human zygote is yet to be confirmed. As patterns form the basis for the evolution of many biological species [36,37], studying standing waves can broaden our understanding of the underlying genesis involved.

Acknowledgements This review arose as a consequence of a workshop on the control of cellular and molecular systems at the Mathematical Biosciences Institute at The Ohio State University, which receives major funding from the National Science Foundation Division of Mathematical Sciences. We are grateful to Yuchuan Miao, Marc Edwards and Peter Devreotes for fruitful conversations and collaboration on wave propagation in migratory cells.

References

1. Bement WM, Leda M, Moe AM, Kita AM, Larson ME, Golding AE, Pfeuti C, Su KC, Miller AL, Goryachev AB, von Dassow G (2015) Activator-inhibitor coupling between rho signalling and actin assembly makes the cell cortex an excitable medium. Nat Cell Biol 17(11):1471–83. https://doi.org/10.1038/ncb3251
2. Bhattacharya S, Iglesias PA (2016) The regulation of cell motility through an excitable network. IFAC-PapersOnLine 49(26):357–363
3. Braune M, Engel H (1993) Compound rotation of spiral waves in active media with periodically modulated excitability. Chem Phys Lett 211(6):534–540
4. Breña-Medina V, Champneys A (2014) Subcritical Turing bifurcation and the morphogenesis of localized patterns. Phys Rev E 90(3):032923
5. Burkitt AN (2006) A review of the integrate-and-fire neuron model: I. homogeneous synaptic input. Biol Cybern 95(1):1–19
6. Cheng H, Lederer MR, Lederer W, Cannell M (1996) Calcium sparks and $[Ca^{2+}]_i$ waves in cardiac myocytes. Am J Physiol Cell Physiol 270(1):C148–C159
7. Dahlem MA, Müller SC (1997) Self-induced splitting of spiral-shaped spreading depression waves in chicken retina. Exp Brain Res 115(2):319–324
8. Davidenko JM, Pertsov AV, Salomonsz R, Baxter W, Jalife J (1992) Stationary and drifting spiral waves of excitation in isolated cardiac muscle. Nature 355(6358):349–351
9. Deneke VE, Di Talia S (2018) Chemical waves in cell and developmental biology. J Cell Biol 217(4):1193–1204
10. Devreotes PN, Bhattacharya S, Edwards M, Iglesias PA, Lampert T, Miao Y (2017) Excitable signal transduction networks in directed cell migration. Ann Rev Cell Dev Biol 33:103–125
11. Dockery J, Keener J (1989) Diffusive effects on dispersion in excitable media. SIAM J Appl Math 49(2):539–566
12. Dockery JD (1992) Existence of standing pulse solutions for an excitable activator-inhibitory system. J Dyn Diff Equat 4(2):231–257
13. Ermentrout G, Hastings S, Troy W (1984) Large amplitude stationary waves in an excitable lateral-inhibitory medium. SIAM J Appl Math 44(6):1133–1149
14. Ermentrout GB, Rinzel J (1996) Reflected waves in an inhomogeneous excitable medium. SIAM J Appl Math 56(4):1107–1128
15. Fife PC (1984) Propagator-controller systems and chemical patterns. In: Vidal C, Pacault A (eds) Non-equilibrium dynamics in chemical systems, pp 76–88. Springer
16. Fife PC (2013) Mathematical aspects of reacting and diffusing systems, vol 28. Springer, Berlin
17. FitzHugh R (1961) Impulses and physiological states in theoretical models of nerve membrane. Biophys J 1(6):445–66
18. Franci A, Sepulchre R (2016) A three-scale model of spatio-temporal bursting. SIAM J Appl Dyn Syst 15(4):2143–2175
19. Gierer A, Meinhardt H (1972) A theory of biological pattern formation. Kybernetik 12(1):30–39
20. Hodgkin AL, Huxley AF (1952) A quantitative description of membrane current and its application to conduction and excitation in nerve. J Physiol 117(4):500–44
21. Holmes WR, Carlsson AE, Edelstein-Keshet L (2012) Regimes of wave type patterning driven by refractory actin feedback: transition from static polarization to dynamic wave behaviour. Phys Biol 9(4):046005
22. Iglesias P (2013) Excitable systems in cell motility. In: 2013 IEEE 52nd annual conference on decision and control (CDC), pp 757–762. Florence, Italy. https://doi.org/10.1109/CDC.2013.6759973

23. Iglesias PA, Devreotes PN (2012) Biased excitable networks: how cells direct motion in response to gradients. Curr Opin Cell Biol 24(2):245–53. https://doi.org/10.1016/j.ceb.2011.11.009
24. Jalife J (2003) Rotors and spiral waves in atrial fibrillation. J Cardiovasc Electrophysiol 14(7):776–780
25. Jones CK, Rubin JE (1998) Existence of standing pulse solutions to an inhomogeneous reaction-diffusion system. J Dyn Differ Equ 10(1):1–35
26. Keener JP (1980) Waves in excitable media. SIAM J Appl Math 39(3):528–548
27. Keener JP (1986) A geometrical theory for spiral waves in excitable media. SIAM J Appl Math 46(6):1039–1056
28. Keener JP, Sneyd J (1998) Mathematical physiology, vol 1. Springer, New York
29. Kondo S, Asai R (1995) A reaction-diffusion wave on the skin of the marine angelfish Pocamanthus. Nature 376(6543):765–768
30. Kosek J, Marek M (1995) Collision-stable waves in excitable reaction-diffusion systems. Phys Rev Lett 74(11):2134
31. Lapique L (1907) Recherches quantitatives sur l'excitation électrique des nerfs traitée comme une polarization. J Physiol Pathol Gen 9:620–635
32. Leppänen T (2005) The theory of Turing pattern formation. In: Barrio RA, Kaski KK (eds) Current topics in physics: in honor of Sir Roger J Elliott, pp 199–227. World Scientific
33. Li G, Ouyang Q, Petrov V, Swinney HL (1996) Transition from simple rotating chemical spirals to meandering and traveling spirals. Phys Rev Lett 77(10):2105
34. Li JH, Haim M, Movassaghi B, Mendel JB, Chaudhry GM, Haffajee CI, Orlov MV (2009) Segmentation and registration of three-dimensional rotational angiogram on live fluoroscopy to guide atrial fibrillation ablation: a new online imaging tool. Heart Rhythm 6(2):231–237
35. Luther S, Fenton FH, Kornreich BG, Squires A, Bittihn P, Hornung D, Zabel M, Flanders J, Gladuli A, Campoy L et al (2011) Low-energy control of electrical turbulence in the heart. Nature 475(7355):235
36. Meinhardt H (1993) A model for pattern formation of hypostome, tentacles, and foot in hydra: how to form structures close to each other, how to form them at a distance. Dev Biol 157(2):321–333
37. Meinhardt H, de Boer PA (2001) Pattern formation in Escherichia coli: a model for the pole-to-pole oscillations of Min proteins and the localization of the division site. Proc Natl Acad Sci USA 98(25):14202–14207
38. Miao Y, Bhattacharya S, Edwards M, Cai H, Inoue T, Iglesias PA, Devreotes PN (2017) Altering the threshold of an excitable signal transduction network changes cell migratory modes. Nat Cell Biol 19(4):329–340
39. Mikhailov A, Davydov V, Zykov V (1994) Complex dynamics of spiral waves and motion of curves. Physica D 70(1–2):1–39
40. Mikhailov AS, Zykov VS (1995) Spiral waves in weakly excitable media. In: Kapral R, Showalter K (eds) Chemical waves and patterns, pp 119–162. Springer
41. Mori Y, Jilkine A, Edelstein-Keshet L (2008) Wave-pinning and cell polarity from a bistable reaction-diffusion system. Biophys J 94(9):3684–3697
42. Morris C, Lecar H (1981) Voltage oscillations in the barnacle giant muscle fiber. Biophys J 35(1):193–213
43. Muller L, Piantoni G, Koller D, Cash SS, Halgren E, Sejnowski TJ (2016) Rotating waves during human sleep spindles organize global patterns of activity that repeat precisely through the night. Elife 5(e17):267
44. Murray JD (2001) Mathematical biology. II spatial models and biomedical applications (Interdisciplinary applied mathematics), vol 18. Springer, New York
45. Murray JD (2002) Mathematical biology. I. (Interdisciplinary applied mathematics), vol 17. Springer, New York
46. Nagumo J, Arimoto S, Yoshizawa S (1962) An active pulse transmission line simulating nerve axon. Proc IRE 50(10):2061–2070
47. Narayan SM, Krummen DE, Shivkumar K, Clopton P, Rappel WJ, Miller JM (2012) Treatment of atrial fibrillation by the ablation of localized sources: confirm (conventional ablation for atrial fibrillation with or without focal impulse and rotor modulation) trial. J Am Coll Cardiol 60(7):628–636
48. Panfilov AV, Keener JP (1993) Effects of high frequency stimulation on cardiac tissue with an inexcitable obstacle. J Theor Biol 163(4):439–448
49. Pertsov AM, Davidenko JM, Salomonsz R, Baxter WT, Jalife J (1993) Spiral waves of excitation underlie reentrant activity in isolated cardiac muscle. Circ Res 72(3):631–650
50. Petrov V, Scott SK, Showalter K (1994) Excitability, wave reflection, and wave splitting in a cubic autocatalysis reaction-diffusion system. Philos Trans R Soc Lond A Math Phys Eng Sci 347(1685):631–642
51. Quail T, Shrier A, Glass L (2014) Spatial symmetry breaking determines spiral wave chirality. Phys Rev Lett 113(15):158101
52. Rinzel J, Terman D (1982) Propagation phenomena in a bistable reaction-diffusion system. SIAM J Appl Math 42(5):1111–1137
53. Showalter K, Tyson JJ (1987) Luther's 1906 discovery and analysis of chemical waves. J Chem Educ 64(9):742
54. Steinbock O, Zykov V, Müller SC (1993) Control of spiral-wave dynamics in active media by periodic modulation of excitability. Nature 366(6453):322–324
55. Takahashi K, Saleh M, Penn RD, Hatsopoulos NG (2011) Propagating waves in human motor cortex. Front Hum Neurosci 5:40
56. Turing AM (1952) The chemical basis of morphogenesis. Philos Trans R Soc Lond B Biol Sci 237(641):37–72
57. Tyson JJ, Keener JP (1988) Singular perturbation theory of traveling waves in excitable media (a review). Physica D 32(3):327–361
58. Vanag VK, Epstein IR (2001) Pattern formation in a tunable medium: the Belousov-Zhabotinsky reaction in an aerosol ot microemulsion. Phys Rev Lett 87(22):228301
59. Verschueren N, Champneys A (2017) A model for cell polarization without mass conservation. SIAM J Appl Dyn Syst 16(4):1797–1830
60. Weiner OD, Marganski WA, Wu LF, Altschuler SJ, Kirschner MW (2007) An actin-based wave generator organizes cell motility. PLoS Biol 5(9):e221. https://doi.org/10.1371/journal.pbio.0050221
61. Wiener N, Rosenblueth A (1946) The mathematical formulation of the problem of conduction of impulses in a network of connected excitable elements, specifically in cardiac muscle. Arch Inst Cardiol Mex 16(3):205–265
62. Wilson D, Moehlis J (2016) Toward a more efficient implementation of antifibrillation pacing. PloS ONE 11(7):e0158239
63. Winfree AT (1972) Spiral waves of chemical activity. Science 175(4022):634–636
64. Winfree AT (2001) The geometry of biological time. In: Interdisciplinary applied mathematics, vol 12. Springer, Berlin
65. Zhabotinsky AM, Eager MD, Epstein IR (1993) Refraction and reflection of chemical waves. Phys Rev Lett 71(10):1526
66. Zykov V (1980) Analytic evaluation of the relationship between the speed of a wave of excitation in a two-dimensional excitable medium and the curvature of its front. Biophysics 25(5):888–892
67. Zykov V, Krekhov A, Bodenschatz E (2017) Fast propagation regions cause self-sustained reentry in excitable media. Proc Nat Acad Sci 114(6):1281–1286